

1988.

²Tsai, Y. L., and Hsieh, K. C., "Comparative Study of Computational Efficiency of Two LU Schemes for Non-Equilibrium Reacting Flows," AIAA Paper 90-0396, Jan. 1990.

³Bilger, R. W., "Turbulent Flows with Non-Premixed Reactants," *Turbulent Reacting Flows*, edited by P. A. Libby and F. A. Williams, Springer-Verlag, New York, 1981, pp. 65-113.

⁴Chen, J.-Y., and Kollmann, W., "Segregation Parameters and Pair-Exchange Mixing Models for Turbulent Nonpremixed Flames," *Twenty-Third Symposium (International) on Combustion*, Combustion Inst., Pittsburgh, PA, 1990, pp. 751-757.

⁵Eggers, J. M., "Turbulent Mixing of Coaxial Compressible Hydrogen-Air Jets," NASA TN D-6487, Sept. 1971.

⁶Evans, J. S., Schexnayder, C. J., and Beach, H. L., "Application of a Two-Dimensional Parabolic Computer Program to Prediction of Turbulent Reacting Flows," NASA TP-1169, March 1978.

⁷Villasenor, R., Chen, J.-Y., and Pitz, R. W., "Modeling Ideally Expanded Supersonic Turbulent Jet Flows with Nonpremixed H_2 -Air Combustion," *AIAA Journal*, Vol. 30, No. 2, 1992, pp. 395-402.

⁸Beach, H. L., "Supersonic Mixing and Combustion of a Hydrogen Jet in a Coaxial High-Temperature Test Gas," AIAA Paper 72-1179, Nov. 1972.

Dynamical Scaling of a Model Unsteady Separating Flow

Mukund Acharya* and Anwar Ramiz†

Illinois Institute of Technology, Chicago, Illinois 60616

Introduction

MODEL experiments have proven to be of considerable value in understanding the physical mechanisms that control the unsteady separation process and the evolution of the vorticity field over surfaces. Francis et al.,¹ for example, studied the flow produced over a symmetric airfoil by an oscillating fence-like spoiler located at midchord on the suction surface. They documented the presence of a dynamically evolving vortical structure that had many of the characteristics of the dynamic stall vortex that is associated with an airfoil in pitching motion. They observed that, for the range of Reynolds numbers and frequencies tested, the vortical structure remained attached to the spoiler during the upstroke and that it grew mainly in the streamwise direction, with the growth rate of the vortex proportional to the square root of the reduced frequency k of spoiler oscillation.

In another model experiment that exhibits some characteristics of the leading-edge separation over unsteady airfoils, Ramiz and Acharya² and Ramiz³ formulated techniques for the nonintrusive detection of flow state that show promise for use in the active control of unsteady separated flows. The experiment documented the unsteady separating flowfield generated by the deployment at constant pitch rate of a spoiler-like flap, with height $h = 4$ cm and a 60-cm span, into the initially attached flow over a flat plate, 60 cm wide and 3.1 m long. The flap, located at $x_0 = 137$ cm from the plate leading edge, had a single ramp-up motion from 0 to 90 deg over a rise time T_0 . The resulting unsteady flow was studied for a Reynolds number range $1.5 \times 10^5 < Re_{x_0} < 2.6 \times 10^6$ and rise times T_0 between 0.06 and 2 s (corresponding to a dimensionless pitch rate $0.001 < a^+ < 0.35$). The formation and growth of the separated region were examined by using a combination of unsteady wall static pressure and flow-direction measurements at several locations downstream of the

flap. A proper understanding of the development of an unsteady flow such as this requires a perspective based on vorticity dynamics. The results of the present experiments are consistent with the suggestion of Reynolds and Carr⁴ that the growth of the separation region is controlled by two different mechanisms that set a balance between the vorticity input and output to the separated region.

Results and Discussion

Nature of the Unsteady Flow

References 2 and 3 provide a detailed description of the measurement techniques and their validity, as well as the results. A sample data set is described here to provide the requisite background for the discussion of dynamical scaling in the following section. Figure 1, reproduced from Ref. 2, shows typical flow-direction data at $x/h = 2$ for five transverse locations ranging between $0.1 < y/h < 4.0$. A zero c_p line for each trace in this figure aids in determining the flow direction at each location; a positive value indicates forward flow. The wall static pressure at this location has also been shown for reference. Several features of the unsteady flow are apparent. Prominent among these is the signature of the initial vortex as it is released from the flap and is convected downstream. This correlation between the occurrence of a suction peak and the vortex passage has been observed in other unsteady flows as well.^{1,5,6} Flow reversal is seen only in the traces recorded at $y/h < 1$. The flow reverses direction first nearest to the wall, with delays occurring in this reversal as y/h increases. Recirculating flow in the separated region forming behind the flap results in reversed flow in the near-wall part of this region. Thus, the existence of reversed flow near the wall at any streamwise location is an indication that the separated region has grown in extent up to this location. Measurements of the direction of flow in the near-wall region along the plate can thus be used to obtain a measure of the streamwise extent of the separated region.

Dynamical Scaling

Data such as those presented in Fig. 1, recorded over a range of T_0 and approach flow velocities, showed that the length and time scales of the separation process depend on T_0 and flow velocity. It was found that the behavior of the flow was determined by the relative magnitudes of two time scales: the rise time of the flap and the time available for the vorticity generated at the flap to accumulate in the separated region developing behind the flap. The growth of the separated region beyond a given streamwise location downstream of the flap was preceded by the convection of the initial vortex past that location. In addition, the time of arrival of the vortex at this location was given by the first instant of flow reversal in the near-wall region. This time instant t_d , when flow reversal was first detected in the near-wall region during a flap-rise

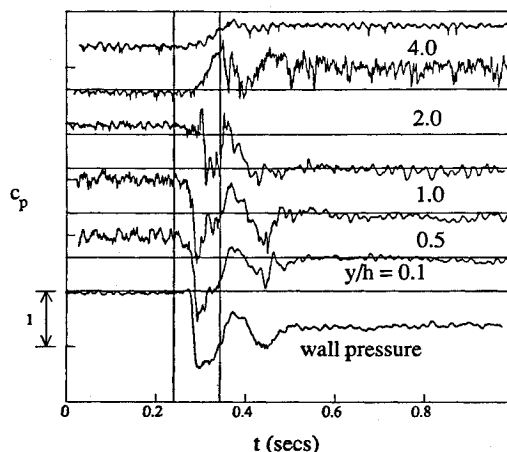


Fig. 1 Typical flow-direction data; $T_0 = 0.1$ s, $Re_{x_0} = 9 \times 10^5$, $x/h = 2$.

Received June 4, 1991; revision received Feb. 19, 1992; accepted for publication Feb. 21, 1992. Copyright © 1992 by the American Institute of Aeronautics and Astronautics, Inc. All rights reserved.

*Associate Professor, Fluid Dynamics Research Center. Member AIAA.

†Graduate Research Assistant, Fluid Dynamics Research Center.

event, could be determined at any location downstream of the flap, either from the flow direction signal or the wall static pressure at this location, measured synchronously with the signature of the flap position.^{2,3} Thus, t_d is a measure of the rate of development of the separated region, and x/t_d is the average velocity at which the separation "front" that divides the outer flow and the recirculating region convects downstream. The t_d may be thought of as the sum of the "hold time," during which the vortex rolls up and is held to the flap, and the time taken to convect downstream following its release from the flap. One would expect that the hold time for quasi-steady conditions would be insignificant and that the convection of the front would be determined solely by the rate at which the flap rose into the flow. Then, at a fixed downstream location, t_d/T_0 would be constant and the time of detection of flow reversal at any location downstream of the flap would be directly proportional to the rise time of the flap. This implies that apart from differences associated with the hold time of the initial vortex, t_d at different streamwise locations should scale with the convective time x/U_∞ .

Detection time data at two locations downstream of the flap, $x/h = 2$ and 5 , were examined for their scaling properties over the parameter range $0.06 \leq T_0 \leq 2.0$ and $9.0 \times 10^5 \leq Re_{x_0} \leq 2.6 \times 10^6$. Figure 2 shows that scaling the detection time data based on the previous observations results in a very good collapse of the data. The abscissa $T_0 U_\infty/h$ is essentially the ratio of the approach flow velocity to the tip velocity of the flap. It may also be thought of as a dimensionless rise time, whose reciprocal would be analogous to a reduced frequency for a periodic motion of the flap. For dimensionless rise times larger than about 100, the variation is linear with a slope of 1, i.e., t_d is determined by the convective process. The unsteady separation behaves in a quasisteady manner in this regime. However, for values of $T_0 U_\infty/h$ less than 100, t_d is larger than would be expected from quasisteady considerations. Under these conditions, the flap has relatively larger tip velocities during its motion into the flow, and unsteady effects become important. The increase in the magnitude of t_d , relative to quasisteady values, is attributable to the proportionately larger hold time of the vortex on the flap before its release and convection downstream. The data in this range follow a power-law variation with an exponent between 0.4 and 0.5. Francis et al. determined the streamwise growth and extent of the recirculation zone by measuring the convection velocity of a phase-averaged vorticity contour and found that the convection velocity exhibited a square-root dependency (exponent = 0.5) on k . Koga⁵ also measured the average convection velocity of the vortical structures generated by an oscillating control

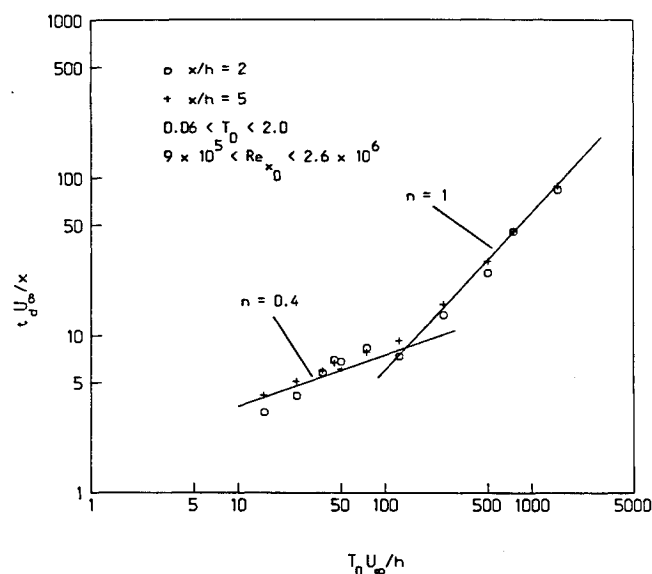


Fig. 2 Scaling of detection time.

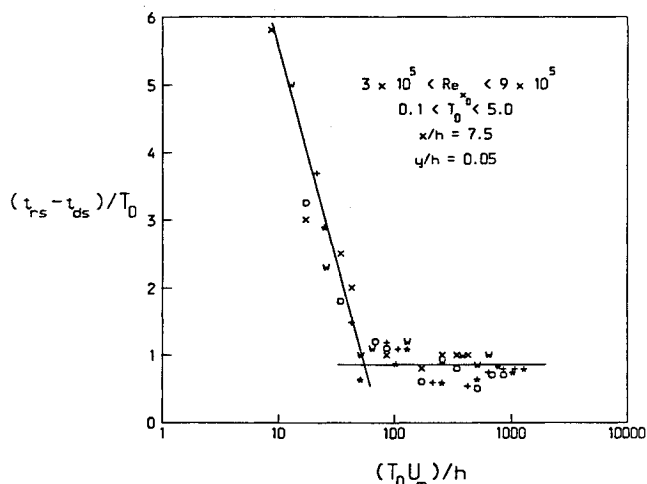


Fig. 3 Scaling of unsteadiness.

flap in a separated flow. A re-examination of his data shows that the convection velocity exhibits a power-law variation with k , with an exponent of 0.4. The data of Francis et al. and Koga did not approach quasisteady conditions. The present results confirm the trends seen in their data at high reduced frequencies and extend those results, providing a clearer characterization of the dependence of the growth of the separated region on the parameters defining the unsteady motion.

The unsteady nature of the developing separated flowfield was examined by monitoring flow direction at a number of streamwise and transverse locations downstream of the flap during its rise. Each of the flow-direction traces so obtained exhibited a certain period of unsteadiness. Sample traces are seen in Fig. 1. The unsteady period was defined as the difference between t_{ds} , the time instant that the signal departed by 3% from an initial mean steady-state value, and t_{rs} , the time instant that the signal settled to within 3% of the final steady-state value, obtained after separation had been established. Figure 3 shows the unsteady time period $(t_{rs} - t_{ds})/T_0$ plotted vs the dimensionless rise time $T_0 U_\infty/h$. The 3% figure was selected after trials with different levels, to find the algorithm that yielded the most consistent results for all of the data recorded. The uncertainty in the results is estimated to be between 5 and 10%, well within the scatter seen in Fig. 3. The data collapse remarkably well and two asymptotic trends are evident. For values of $T_0 U_\infty/h$ greater than about 100, the separating flow exhibits quasisteady behavior, with the unsteady period approximately equal to the rise time of the flap. Below this value, the data also collapse very well, with the time of unsteadiness increasing sharply as the dimensionless rise time is reduced. For the range of parameters investigated, the largest magnitude of this unsteady period was around six flap rise times. An accurate knowledge of this "relaxation time" can be of considerable importance in many technological applications.

The "critical" value of the parameter $T_0 U_\infty/h$ (≈ 100 , corresponding to a dimensionless pitch rate a^+ of 0.016) separates flow regimes with different behavior. Two different mechanisms control the growth of the separation region in these regimes. For large dimensionless rise times (small pitch rates), the vorticity generated at the tip of the flap is drawn gradually and continuously into the reversed-flow region, and the growth of the separation region is linear. For rise times smaller than the critical value, a more complex vorticity balance dictates the growth rate of the separated region. Miao et al.⁶ recently carried out experiments similar to those of Francis and his co-workers, examining the evolution and motion of vortical structures generated by oscillating a vertical spoiler in and out of a turbulent boundary layer. They found that, below a value of reduced spoiler oscillation frequency $k = 0.009$, the growth and convection of the vortical structures

were quasisteady. For values larger than 0.009, they observed that the roll-up time, growth, and release of the periodic vortical structures were strongly dependent on the oscillation frequency. This is consistent with the present results.

Acknowledgment

This work was supported by the Air Force Office of Scientific Research under Contract F49620-86-0133, monitored by H. Helin.

References

- ¹Francis, M. S., Keese, J. E., Lang, J. D., Sparks, G. W., Jr., and Sisson, G. E., "Aerodynamic Characteristics of an Unsteady Separated Flow," *AIAA Journal*, Vol. 17, No. 12, 1979, pp. 1332-1339.
- ²Ramiz, M. A., and Acharya, M., "The Detection of Flow State in an Unsteady Separated Flow," *AIAA Journal*, Vol. 30, No. 1, 1992, pp. 117-123.
- ³Ramiz, M. A., "The Development of a Simple, Non-Intrusive Technique for Flow-State Detection in a Model, Leading-Edge Unsteady Separation," M.S. Thesis, Mechanical and Aerospace Engineering Dept., Illinois Inst. of Technology, Chicago, IL, May 1989.
- ⁴Reynolds, W. C., and Carr, L. W., "Review of Unsteady, Driven, Separated Flows," *AIAA Paper 85-0527*, March 1985.
- ⁵Koga, D. J., "Control of Separated Flowfields Using Forced Unsteadiness," Ph.D. Dissertation, Mechanical and Aerospace Engineering Dept., Illinois Inst. of Technology, Chicago, IL, 1983.
- ⁶Miau, J., Chen, M., and Chou, J., "Frequency Effect of an Oscillating Plate Immersed in a Turbulent Boundary Layer," *AIAA Paper 89-1016*, March 1989.

Efficient Iterative Methods for the Transonic Small Disturbance Equation

A. S. Lyrintzis,* A. M. Wissink,†
and A. T. Chronopoulos‡
University of Minnesota,
Minneapolis, Minnesota 55455

Nomenclature

A	= term defined in Eq. (3)
b	= right-hand-side vector
C	= coefficient matrix of system of equations
c_1, c_2	= constants defined in Eqs. (6)
D_x	= operator defined in Eqs. (6)
F, F'	= functions used in Newton's method, Eq. (7)
f	= intermediate value for the velocity potential
g	= airfoil surface shape function
M_∞	= freestream Mach number
$u, \hat{u}, \bar{u}, \tilde{u}$	= velocities defined in Eqs. (6)
γ	= ratio of specific heats
δ, Δ	= difference operators defined in Eqs. (6)
ϵ	= switching flag
τ	= airfoil thickness
Φ	= disturbance velocity potential

Subscripts

i, j	= x and y coordinates of solution mesh
x, y	= direction for difference operators d and D

Received Nov. 15, 1991; revision received Feb. 13, 1992; accepted for publication Feb. 28, 1992. Copyright © 1992 by A. S. Lyrintzis, A. M. Wissink, and A. T. Chronopoulos. Published by the American Institute of Aeronautics and Astronautics, Inc., with permission.

*Assistant Professor, Department of Aerospace Engineering and Mechanics. Member AIAA.

†Graduate Research Assistant, Department of Aerospace Engineering and Mechanics. Student Member AIAA.

‡Assistant Professor, Department of Computer Science.

Superscript

n = iteration number

Introduction

THE steady two-dimensional transonic small disturbance (TSD) equation is solved using a new method. Approximate factorization techniques^{1,2} traditionally have been used for the solution of this equation. Other methods have used finite difference techniques to discretize the nonlinear TSD equation, approximate factorizations to achieve linearization, and alternating direction implicit (ADI) techniques to solve the resulting linear tridiagonal systems.

In this Note we present a different method of solving the TSD equation. After the finite difference discretization, we use a Newton method to solve the resulting nonlinear system of equations. Conjugate gradient methods can be used for the solution of the linear system of equations in each time step. These methods are fully vectorizable and very efficient. In this work we used a preconditioned algorithm called Orthomin.³ An efficient parallel and vector implementation of Orthomin appears in Ref. 4. The preconditioning method used incomplete LU decomposition (ILU), is obtained from the incomplete factorization of the matrix, proposed by Meijerink and van der Vorst.⁵ We use a vectorizable version of ILU.⁴ The idea of using Newton's method in transonic flow is not new. Hafez and Palaniswamy⁶ used a direct system solver for each Newton step. The method presented here (i. e., Orthomin with ILU preconditioner) is much more efficient.

The two algorithms (ADI and Newton-Orthomin) were implemented for different test cases. We looked at subsonic and transonic flowfields for a parabolic and a NACA 64A006 airfoil for different mesh sizes. Both algorithms gave the same accuracy, but the iterative method yields better efficiency.

Theoretical Development

The TSD equation for two-dimensional steady flow can be written as

$$\left[\frac{1 - M_\infty^2}{\tau^{3/2}} - (\gamma + 1) M_\infty^2 \Phi_x \right] \Phi_{xx} - \Phi_{yy} = 0 \quad (1)$$

The far-field boundary conditions applied to the problem are $\Phi = 0$ along the left, right, and top edges of the mesh. The flow tangency condition is applied along the surface of the airfoil. Thus, the conditions applied along the bottom of the mesh ($y = 0$) are

$$\frac{\partial \Phi}{\partial y} = \frac{\partial g}{\partial x} \text{ along airfoil, } \Phi = 0 \text{ elsewhere} \quad (2)$$

Equation (1) is discretized with finite differences over a solution mesh. The mesh used is normalized with the chord length of the airfoil, extending five chord lengths in both the x and y directions. A nonuniform (80×30) mesh is used for most tests, but a finer (160×60) mesh is also tested. Only half of the physical region of the airfoil is needed since only symmetric airfoils are studied.

For notation purposes, we define the parameter

$$A = \left[\frac{1 - M_\infty^2}{\tau^{3/2}} - (\gamma + 1) M_\infty^2 \Phi_x \right] \quad (3)$$

The value of A is important because it governs the switching procedure from subcritical to supercritical flow. When A is positive, Eq. (1) is elliptic (subsonic flow) and the equation can be solved using Eq. (1) and central differences for Φ_{xx} and Φ_{yy} . However, when A is negative, Eq. (1) is hyperbolic (supersonic flow) and must be solved using backward differences. Murman's switch (approximate factorization two, AF2 code) was used initially with good results.⁷ Here we present a more advanced monotone switch that was introduced by Goorjian